Accommodating a 650 GeV scalar resonance in HEFT

Iñigo Asiáin,[*] Domènec Espriu,[†] and Federico Mescia[‡]
Departament de Física Quàntica i Astrofísica, Institut de Ciències del Cosmos (ICCUB), Universitat de Barcelona, Martí Franquès 1, 08028 Barcelona, Spain

(Received 15 June 2023; accepted 14 August 2023; published 13 September 2023)

Loss of unitarity in an effective field theory is often cured by the appearance of dynamical resonances, revealing the presence of new degrees of freedom. These resonances may manifest themselves when suitable unitarization techniques are implemented in the effective theory, which in the scalar-isoscalar channel require making use of the coupled-channel formalism. Conversely, experimental detection of a resonance may provide interesting information on the couplings and constants of the relevant effective theory. By applying the systematic procedure developed in previous works, we will attempt to accommodate a possible scalar resonance with mass around 650 GeV for which there is preliminary evidence at the LHC in the vector-boson fusion channel. The results are interesting; the resonance can be accommodated within the experimentally allowed range of next-to-leading order coefficients in the Higgs effective field theory but in a rather nontrivial manner. Interestingly, its width and production cross section turn out to agree with the tentative experimental results.

DOI: 10.1103/PhysRevD.108.055013

I. INTRODUCTION

The presence of new particles at the LHC would be a clear indication of the existence of new physics beyond the Standard Model (SM). The masses of these yet undiscovered states could suggest a scale of new physics, to be explored, and their production channel would provide a guidance for future-experiment proposals. However, after the discovery in 2012 of a Higgs-like particle, the $h(125)$, so far compatible with the minimal SM, there have been no clear signals of new findings regarding this matter.

There is an obvious interest in the appearance of (relatively) light scalar companions of the $h(125)$ as they may arise in composite Higgs models (see, e.g., Ref. [1] and the references therein) as (pseudo-)Goldstone-like spare states following the spontaneous symmetry breaking (SSB) of the vacuum of a theory possessing a larger global symmetry group. Other models try to explain such triggering of the electroweak symmetry breaking sector (EWSBS) with more than one scalar such as the Georgi-Machacek [2], Chanowitz-Golden [3], and two-Higgs-doublet (2HDM) [4] models. In Ref. [5], a list of scalar resonances such as H(650), $A(400)$, $h(151)$, and $h(95)$ and their statistical significance is presented with conclusive results for the particular case of H(650) claiming a 7 standard deviation global significance coming from combined analysis in various channels. Another scalar state $h'(515)$ is treated in Ref. [6] assuming an holographic description of a strong sector beyond-the-SM (BSM).

In Refs. [7,8] we saw, in the context the Higgs effective field theory (HEFT), how resonant states appear at the scale of unitarity violation of the perturbative amplitudes for certain ranges of the effective couplings. The inverse amplitude method (IAM), which is derived from analytical properties of partial waves in the s-complex plane, is the tool of choice employed to understand the emergence of dynamical resonances. In the case of the $IJ = 00$ channel, where the $h(125)$ belongs, the analysis is more involved than when searching for vector resonances due to the need for making use of the coupled channel formalism. A rather detailed exploration of possible scalar resonances and their implication for the HEFT coefficients was carried out in Ref. [8] but was restricted to resonances heavier that 1.8 TeV. This restriction arises from the need of fulfilling various phenomenological constraints for vector resonances [9]. However, pseudo-Goldstone bosons in the scalar channel may be lighter and it is therefore appropriate to examine the possible presence of light states.

Recently, some interest has emerged on a possible signal for a Higgs-like state around 600 GeV, much below the region just mentioned. Searches in CMS [10] and ATLAS [11] (see Refs. [12,13] for a combined analysis) have yielded some evidence for the production of this resonance

[*]iasiain@icc.ub.edu
[†]espriu@icc.ub.edu
[‡]mescia@ub.edu

through the clear four-leptonic final state; $\mathrm{H}(650) \to ZZ \to 4l$. In particular, they suggest a scalar state peaking at ∼650 GeV with a total width of approximately 100 GeV, with a 3.75σ significance using an integrated luminosity of 139 fb^{-1}. The corresponding cross section for the subprocess $pp \to ZZ + X$ is 90 ± 25 fb. After applying sequential cuts, an ATLAS analysis for vector boson fusion [11] reduces the significance of this resonance to 2.1σ and the cross section to 30 ± 15 fb, significantly below the inclusive one before the cuts. On the other hand, searches of leptonic decays from WW ($2l$ + missing energy) enhances the production rate for this scalar to more than five times the ZZ one, resulting in a cross section of 160 ± 50 fb. This scenario of unbalanced production rates between channels will actually be reproduced in our HEFT description, as we will see. The question that naturally emerges is; is such a light resonance compatible with existing bounds on the low-energy coefficients of the HEFT? This is not obvious at all, because strict bounds already exist on many of these coefficients as we will see below. These bounds place various such coefficients in the 10^{-4} range, which typically provide resonances above the TeV scale, but several other couplings are poorly bounded or not bounded at all. Can therefore the H(650) be accommodated in the HEFT without violating any existing bounds? This seems a relevant question because a negative answer—taking into account the generality of the HEFT approach—would most likely give credibility to the experimental hints.

In Sec. II we present the theoretical framework we use, namely the HEFT, with all the considerations we have taken in order to simplify the computation of the relevant $2 \to 2$ processes at the one-loop level. We also include information regarding the experimental status of the couplings that define the relevant parameter space for our purposes. To finish this section we will succinctly comment on the systematics needed to build the partial waves that will be rendered unitary. The interested reader may find much more detailed information in Ref. [8].

Section III will be devoted to the analysis of the HEFT parameter space selected by a H(650)-like resonance in WW unitarized scattering.

Some previous works have already studied models with states similar to H(650) [2–6,12,13].

II. EFFECTIVE LAGRANGIAN, EXPERIMENTAL BOUNDS, AND PARTIAL WAVES

In this section we will summarize our notation and, in particular, identify the low-energy constants called to play a role in the subsequent analysis. Following previous studies in Refs. [7,8] regarding vector and scalar resonances we work in the framework of the HEFT, an $SU(2)_L \times SU(2)_R$ symmetric chiral Lagrangian with the addition of a light Higgs with mass $M_h = 125\,\mathrm{GeV}$, and under the assumption that the custodial symmetry remains exact after the spontaneous breaking of the vacuum of the theory following the pattern $SU(2)_L \times SU(2)_R \to SU(2)_V$, therefore neglecting the soft breaking induced by $\mathcal{O}(g')$ pieces gauging the $U(1)_Y$ subgroup. Consequently, we set $g' = 0$ and the purely electromagnetic effects that make the W and Z gauge bosons masses differ are absent; W and Z transform exactly as a triplet under the custodial group (we will refer to them indistinctly as W) and there are no vertices involving photons whatsoever. This simplification, useful to employ an exact weak isospin formalism, is not expected to have any significant effect on the analysis.

The HEFT is constructed as an expansion in powers of the momentum (derivatives) and, in clear contrast to the linear case where order-by-order suppression is performed by explicit powers of an energy cutoff in the denominator to obey canonical dimensional analysis, the chiral order of any operator represents the number of derivatives and/or soft mass scales M_W ($\sim g$) and M_H ($\sim\sqrt{\lambda}$) that it contains. Up to $\mathcal{O}(p^4)$ we need the following pieces:

$$\begin{aligned}\mathcal{L}_2 =& -\frac{1}{2g^2}\mathrm{Tr}(\hat{W}_{\mu\nu}\hat{W}^{\mu\nu}) - \frac{1}{2g'^2}\mathrm{Tr}(\hat{B}_{\mu\nu}\hat{B}^{\mu\nu}) \\ &+ \frac{v^2}{4}\mathcal{F}(h)\mathrm{Tr}(D^\mu U^\dagger D_\mu U) + \frac{1}{2}\partial_\mu h \partial^\mu h - V(h), \qquad (1)\end{aligned}$$

$$\begin{aligned}\mathcal{L}_4 =& -i a_3 \mathrm{Tr}(\hat{W}_{\mu\nu}[V^\mu, V^\nu]) + a_4(\mathrm{Tr}(V_\mu V_\nu))^2 \\ &+ a_5(\mathrm{Tr}(V_\mu V^\mu))^2 + \frac{\delta}{v^2}(\partial_\mu h \partial^\mu h)\mathrm{Tr}(D_\mu U^\dagger D^\mu U) \\ &+ \frac{\eta}{v^2}(\partial_\mu h \partial_\nu h)\mathrm{Tr}(D^\mu U^\dagger D^\nu U) \\ &+ \frac{\gamma}{v^4}(\partial_\mu h \partial^\mu h)^2 + i\frac{\zeta}{v}\mathrm{Tr}(\hat{W}_{\mu\nu}V^\mu)\partial^\nu h, \qquad (2)\end{aligned}$$

with the building blocks

$$\begin{aligned}&U = \exp\left(\frac{i\omega^a\sigma^a}{v}\right), \quad \mathcal{F}(h) = 1 + 2a\left(\frac{h}{v}\right) + b\left(\frac{h}{v}\right)^2 + \ldots, \\ &D_\mu U = \partial_\mu U + i\hat{W}_\mu U, \quad \hat{W}_\mu = g\frac{\vec{W}_\mu\cdot\vec{\sigma}}{2}, \quad V_\mu = D_\mu U^\dagger U, \\ &V(h) = \frac{1}{2}M_h^2 h^2 + d_3\lambda v h^3 + d_4\frac{\lambda}{4}h^4 + \ldots, \\ &\hat{W}_{\mu\nu} = \partial_\mu\hat{W}_\nu - \partial_\nu\hat{W}_\mu + i[\hat{W}_\mu, \hat{W}_\nu]. \qquad (3)\end{aligned}$$

The effective Lagrangian suitable for our purposes is then

$$\mathcal{L} = \mathcal{L}_2 + \mathcal{L}_4 + \mathcal{L}_{GF} + \mathcal{L}_{FP}, \qquad (4)$$

where the last two pieces are the gauge-fixing and the associated Faddeev-Popov, respectively, that are trivial (induce no dynamics) in the Landau gauge ($\xi = 0$) with massless Goldstones that we use throughout.

The deviations from the SM are parametrized by the—often called anomalous—couplings accompanying the local operators in Eqs. (1) and (2). Any BSM model can

be reproduced by a suitable choice of these anomalous couplings in the HEFT. The SM corresponds to a particular choice of the couplings, namely $\alpha_{p^2}=1$ and $\alpha_{p^4}=0$ where α_{p^k} generically represents the full set of chiral parameters belonging to the Lagrangian $\mathcal{L}_k$, this is, of chiral order k. The reverse is not true; random values for the anomalous couplings will typically lead to inconsistencies, such as lack of causality [14], and cannot correspond to any meaningful UV completion.

We will restrict the possible values of the anomalous couplings by making use of the experimental bounds available up to date and the hierarchy of the effects that they produce in our results. As a working hypothesis, we will assume that all α_{p^2} couplings take their canonical SM values and, consequently, departures will be described by anomalous values of the α_{p^4}. Regarding the latter, it is easy to see to see why considering a_3 and ζ will have a subleading role; they are couplings that enter at $\mathcal{O}(p^4)$, just like $a_4, a_5\cdots$, but they have one derivative less [they are $\mathcal{O}(g)$ instead] which translates into one power less of momenta easing their high-energy contribution in comparison to operators with four derivatives. Thus, we will not take them into account in our analysis.

From an experimental point of view, some of the couplings happen to be poorly restricted, or not restricted at all in the existing literature. In particular we will admit values of the couplings in $\mathcal{L}_4$ in the range [15]

$$a_4\in(-0.0061,0.0063),\qquad a_5\in(-0.0094,0.0098),\quad(5)$$

that have been obtained using 13 TeV LHC data in four leptons final states from WW/WZ scattering.[1] There is a more strict bound (by a factor 10 [17]) for a_5 coming from an SMEFT analysis with $2l2j$ final states, much lesser clear channel. However, it should be noted that in the scalar-isoscalar channel the couplings a_4 and a_5 always appear in the combination $5a_4+8a_5$ and therefore the error in a_4 amply dominates anyway.

As said, the rest of the α_{p^4} couplings relevant for the present discussion, namely δ, η, and γ, remain unconstrained experimentally, but taking into account the fact that they are absent in the SM, we will allow these to have a maximum (absolute) value of 10^{-3}.

[1]In [15], the bounds are worked out in the SMEFT basis and are for the (dimensionful) coefficients $f_{S,i}/\Lambda^4$ $(i=\{0,1,2\})$. Then, in the HEFT basis

$$a_4=\frac{v^4}{8}\frac{f_{S,0}}{\Lambda^4}\Big|,\qquad a_5=\frac{v^4}{16}\frac{f_{S,1}}{\Lambda^4}.$$

Follow discussion in Ref. [7] for more details. In Ref. [16], the bounds are directly for $a_{4,5}$ couplings with the K-matrix unitarization method. However, the analysis does not fully leverage yet the available LHC statistics. Consequently, the a_4 and a_5 bounds are about four times weaker than the ones shown in Eq. (5).

As anticipated in the introduction the amplitudes coming from the Lagrangian (4) lack unitarity, being fast growing with the center of mass energy, unless all couplings are taken equal to their SM value. This fact has to be addressed if one wants to make predictions using an effective theory that somehow keeps track of the physical UV behavior of the complete theory from which it supposedly comes from. Hence, unitarization methods are required beyond a certain energy range. Among the various unitarization techniques we will be using the IAM that has been proven to show the same qualitative results that the others and the unitarized amplitudes match, by construction, the perturbative ones at low energies, before unitarity is manifestly lost.

The IAM is implemented in amplitudes with well-defined angular momentum and weak isospin quantum numbers, an IJ basis. A way to build this amplitudes, and in particular the isoscalar-scalar ($IJ=00$) we are interested in, is presented in Ref. [7] and it turns out to be greatly simplified in our custodial limit making use of Bose and crossing symmetries.

The result for the unitarized partial wave is

$$t_{IJ}^{IAM}=t_{IJ}^{(2)}\cdot\left(t_{IJ}^{(2)}-t_{IJ}^{(4)}\right)^{-1}\cdot t_{IJ}^{(2)}$$
$$t_{IJ}^{(n)}=\frac{1}{64\pi}\int_{-1}^{+1}d\cos\theta T_I^{(n)}(s,\cos\theta)P_J(\cos\theta),\quad(6)$$

which at next-to-leading (NLO) precision, the formula for t^{IAM} coincides for both vector and tensor, where $t_{20}^{(n)}$ and $t_{11}^{(n)}$ are functions of s-complex values, and $t_{00}^{(n)}$ that are matrices containing the coupled channels. The expressions to relate the fixed-isospin amplitudes, T_I, with the amplitudes in the charged basis are gathered in Ref. [8].

III. H(650) VIA VBF IN THE HEFT

The exercise we want to do in this section is to search for a set of α_{p^4} HEFT parameters that lead to the presence of a resonance with the properties of the H(650) in WW scattering that are tentatively claimed in Ref. [5]. Though the coupled channel formalism [8], the elastic WW channel is also coupled to both $WW\to hh$ and $hh\to hh$ at the level of unitarized scalar waves. Experimentally, this resonance appears to have a total width of ∼100 GeV, so we focus on the production of a scalar resonance whose mass lies within the 600–700 GeV range.

The anomalous parameters of chiral order two are all set to their SM values; $\alpha_{p^2}=1$. This leaves us with free a_4, a_5, δ, η, and γ. All of them intervene at the NLO (formally tree level) contributions for different processes; the first two to WW elastic scattering, γ to elastic hh and δ and η to the crosses channel $WW\to hh$. However, these separated contributions mix among themselves along the unitarization process.

Following the results in Ref. [8], when we set $\alpha_{p^2}=1$ there are only two physical situations for any choice of the

α_{p^4} chiral parameters; a nonresonant scenario with the absence of any complex pole in the unitarized amplitude, or a resonant one with only one such pole. Whenever there are two poles, one is identified as nonphysical by the phase shift criteria (lies on the first Riemann sheet in the complex s plane). Secondly, the resonances emerging are much more visible in the WW channel than in the coupled ones so the $a_4 - a_5$ plane is the most sensible parameter space to represent the results. As already mentioned in a previous section, this plane is restricted by the experimental bounds quoted in Eq. (5).

In Fig. 1 we show the regions in $a_4 - a_5$ parameter space where a resonance with mass between 600–700 GeV appears using different selection of the α_{p^4} chiral parameters. The different areas are obtained by activating different sets of the NLO HEFT coefficients besides a_4 and a_5, with maximum values of $|10^{-3}|$, following the explanation in the legend. It should be clarified that all the regions overlap with each other: the red one includes the rest of the areas, and the blue one the smaller one in green.

In fact, no bound state with the expected characteristics appears assuming nonzero values for a_4 and a_5 only. One needs the help of at least one more anomalous coupling.

The Fig. 1 above shows regions in the main parameter space where resonances with masses in the range 600–700 GeV are allowed but it says nothing about their properties. One thing that we can indeed extract from Fig. 1 is that the inclusion of δ and η does not affect very much the results when looking for light resonances. With

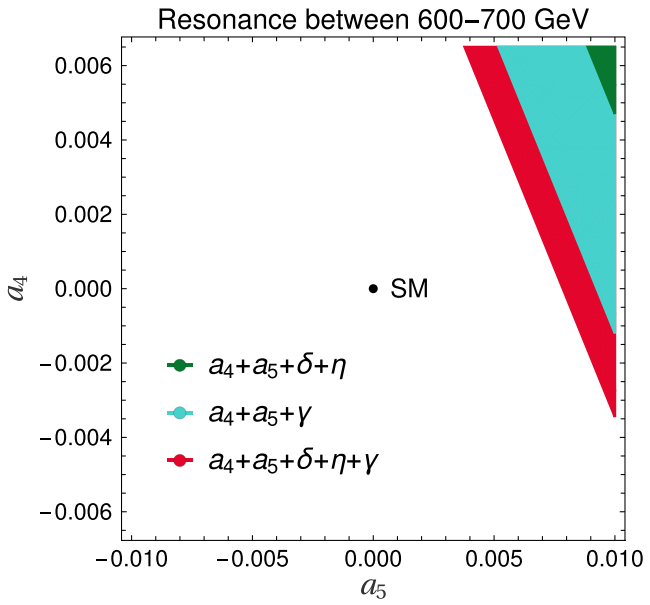

FIG. 1. Regions in the $a_4 - a_5$ plane allowed by experimental constraints where resonances between 600–700 GeV appear when activating different NLO chiral couplings. The more parameters one activates, the less restriction in the plane to achieve the desired scalar light resonance. The LO parameters of Eq. (1) are set to the corresponding SM values.

these, we now investigate the physical properties of the resonances using only a_4, a_5, and γ. Actually, these *a priori* independent three parameters are reduced to two when studying scalar resonances since, as said before, the lines $5a_4 + 8a_5 = k$ contain resonances with the same properties for a fixed k. We choose $k \in (0.055, 0.11)$ so we lie within the pure scalar region, not vector nor tensor states appear, and the experimental bounds in Eq. (5) are satisfied.

In Fig. 2 we show the results. As one can observe, no scenario with negative values of γ exhibits physical resonances: the dashed region is forbidden by the emergence of a second pole identified as nonphysical using the phase-shift criteria and below this area, a nonresonant region appears. Positive values of γ that are not colored in Fig. 2 also lead to physical resonances heavier than 700 GeV, though, so they are excluded from our analysis. Another interesting thing we have observed in the right panel is that for a specific value of γ the width remains constant along the lines $5a_4 + 8a_5 = k$ in the region of interest and they are relatively small (with respect to the masses) leading to quite stable intermediate states emerging in WW scattering. This feature can be explained with the information provided in Ref. [8], where we observed that for large (yet natural) values of $\gamma(\sim 10^{-3})$, the single-channel resonance, this is ignoring coupled-channels, was recovered.

All in all, we have been able to reproduce a scalar resonance with mass around 650 GeV in the HEFT using SM values of the LO Lagrangian and deviations at the next-to-leading order in chiral counting that are within the existing experimental bounds up to date. The more relevant couplings to describe such a resonance happen to be those driving the elastic NLO processes, a_4, a_5, and γ with subleading effects with the off-diagonal ones, δ and η, along the coupled-channel unitarization process. The widths obtained for those new states are quite small compared to their masses, 30–65 GeV.

However, up to now, the more data the experiment collects the more compatible the anomalous couplings are with the successful SM. The BSM H(650)-like resonances in this study appear close to the upper limit of the experimental bounds in Eq. (5), see Fig. 1, meaning that a possible future improvement in these bounds pointing towards consolidation of the SM values would imply their exclusion.

IV. COMPARISON WITH LITERATURE

Detailed information regarding the H(650) can be found in Ref. [5]. In this section we connect these tentative results with the ones extracted from our analysis. We will work under the assumption that the resonant profile obtained, if any, is produced by a single resonance, neglecting the possibility of two overlapping resonances. Besides, we also ignore the decay mode $\mathrm{H}(650) \to h(125)h(95)$, being $h(125)$ the Higgs described in the minimal SM. One way to search for H(650) in vector boson fusion is via the decay to

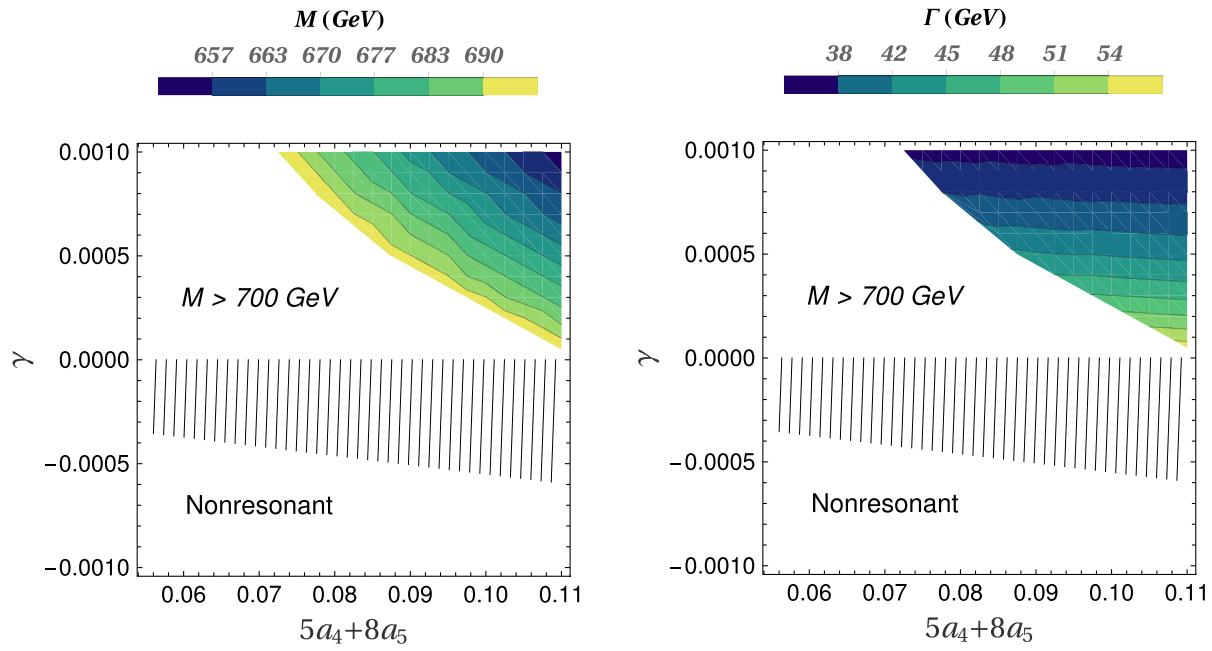

FIG. 2. Masses (left panel) between 600 GeV and 700 GeV and widths (right panel) of scalar resonances in the plane described by the set of lines $5a_4 + 8a_5 = k$ and γ. All negative values of γ are nonphysical (stripped area) by the phase-shift criteria or nonresonant. Positive values of γ below the colorful region exhibit physical resonances, too, but they are heavier than 700 GeV so they are of no interest for this work. The right panel shows how for a fixed value of γ, the widths of the corresponding resonances are independent of the combination $5a_4 + 8a_5$.

$b\bar{b}\gamma\gamma$, but there is yet not enough resolution in the experiment to distinguish between a $b\bar{b}$ pair decayed from a Z or a hypothetical $h(95)$. In other words, we ignore the possible presence of the $h(95)$ that seems less motivated. The interested reader may find this scalar decay in Ref. [18] in the context of 2HDM. This is why for this work we assume the decay mode of H(650) to be exclusively via gauge bosons (however, do keep in mind that other channels contribute in the unitarization procedure).

In Ref. [5], the authors gave a total width to gauge bosons of $\Gamma = 90 \pm 28$ GeV, of the order of the widths presented in the right panel of Fig. 2.

To get a first estimate of the cross section for the production of such resonance we will use the effective W approximation (EWA) [19], which takes Ws and Zs as proton constituents and it is approximately valid for energies well above the EW scale. Within the EWA approach the differential cross-section is given by

$$\frac{d\sigma}{dM_{WW}^2} = \sum_{i,j} \int_{M_{WW}^2/s}^1 \int_{M_{WW}^2/(x_1 s)}^1 \frac{dx_1 dx_2}{x_1 x_2 s} f_i(x_1,\mu_F) f_j(x_2,\mu_F) \times \frac{dL_{WW}}{d\tau} \int_{-1}^1 \frac{d\sigma_{WW}}{d\cos\theta} d\cos\theta \tag{7}$$

with s is the center of mass energy of the two opposite protons at the LHC and M_{WW} is the invariant mass of the two Ws. Here the "partonic" differential cross section in the WW rest frame is

$$\frac{d\sigma_{WW}}{d\cos\theta} = \frac{|A(M_{WW}^2, \cos\theta)|^2}{32\pi M_{WW}^2}, \tag{8}$$

This expression factorizes both energy scales; the one for the long-distance nonperturbative part describing the dynamics inside the proton and a perturbative one for the WW hard scattering.

The amplitude $A(M_{WW}^2, \cos\theta)$ appearing in Eq. (7) describes the amplitude of a WW scattering in the charged (physical) basis that is detected at the LHC and not the amplitude in the IJ basis that we rendered unitary. Thus, by moving backwards along the process we used for unitarization, we have to recover the "unitary" physical amplitude that would produce such a unitary partial wave. From now on, a superindex $\mathcal{U}$ will refer to unitarized quantities, in our case obtained thorough IAM. This is done by reversing the unitarization procedure in Eq. (6)

$$T_I^{\mathcal{U}} = 32\pi \sum_{J=0}^{\infty} (2J+1) t_{IJ}^{\mathcal{U}} P_J(\cos\theta) \tag{9}$$

and we truncate the infinite series at the leading order (LO) for every isospin channel assuming that is a good approximation close to the resonance mass where the peak dominates the amplitude:

$$\begin{aligned} T_0^{\mathcal{U}} &\approx 32\pi t_{00}^{\mathcal{U}}, \\ T_1^{\mathcal{U}} &\approx 32\pi (3 t_{11}^{\mathcal{U}} \cos\theta), \\ T_2^{\mathcal{U}} &\approx 32\pi t_{20}^{\mathcal{U}}. \end{aligned} \tag{10}$$

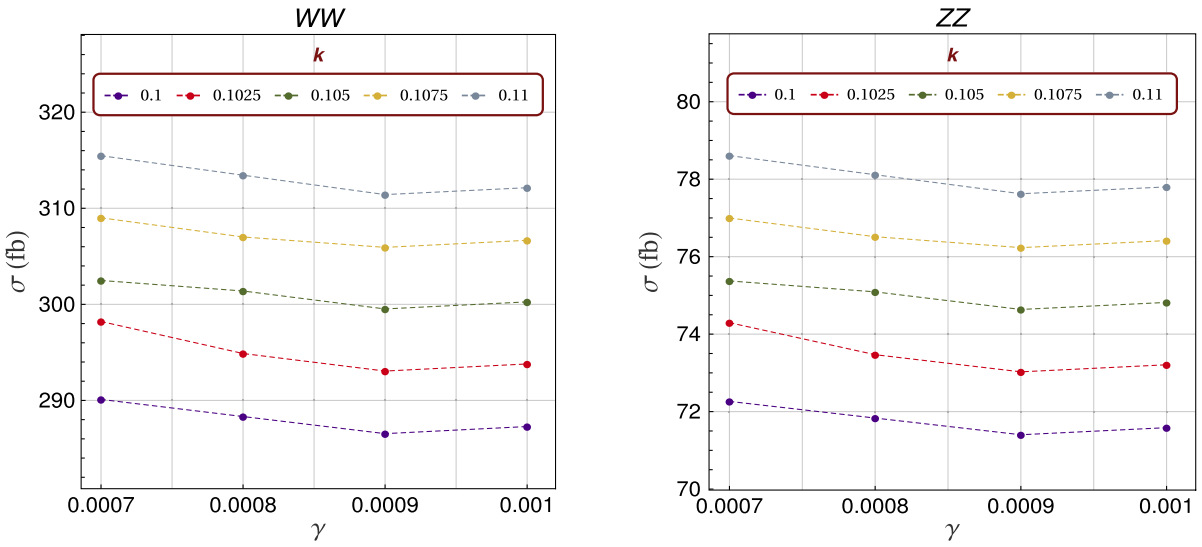

FIG. 3. Values for the VBS cross section in Eq. (13) with WW (left) and ZZ (right) final states versus the NLO chiral parameter γ and for different values of $k = 5a_4 + 8a_5$ in the legend. The combination of the values of k and γ present in the figure make up the top-right region of Fig. 2 where resonances close to 650 GeV appear. The center of mass energy for this calculation is set to $\sqrt{s} = 13$ TeV.

Now, we simply use the isospin relation to build the "unitary" physical amplitudes. We will be using for comparison with the literature those with WW and ZZ in the final states after vector boson scattering (VBS):

$$\begin{aligned} A^{\mathcal{U}}(W^+W^- \to W^+W^-) &= \frac{1}{3}T_0^{\mathcal{U}} + \frac{1}{2}T_1^{\mathcal{U}} + \frac{1}{6}T_2^{\mathcal{U}}, \\ A^{\mathcal{U}}(W^+W^- \to ZZ) &= \frac{1}{3}T_0^{\mathcal{U}} - \frac{1}{3}T_2^{\mathcal{U}}, \\ A^{\mathcal{U}}(ZZ \to ZZ) &= \frac{1}{3}T_0^{\mathcal{U}} + \frac{2}{3}T_2^{\mathcal{U}}, \end{aligned} \tag{11}$$

and the symmetric processes under time reversion.

The EWA consists in convoluting the probability for a quark inside a proton to radiate a gauge boson with the actual parton distribution function (pdf) for the constituent quarks q at some energy scale, $f_q(x,\mu)$, using the effective[2] luminosity [21]

$$\frac{dL_{WW}}{d\tau} = \left(\frac{g}{4\pi}\right)^4 \left[\left(\frac{1}{\tau}+1\right)\ln\left(\frac{1}{\tau}\right) - 2\left(\frac{1}{\tau}-1\right)\right], \tag{12}$$

where $\tau = M_{WW}^2/(x_1x_2s)$ connects both energy scales. A factor $1/2$ must be added for ZZ final states accounting for their indistinguishability.

After performing the convolution of these functions we are in disposition to compute the integral in Eq. (7) to obtain the differential cross section of the process with respect to the invariant mass of the WW system. Moreover, the total cross section of the process is obtained assuming that the peak indeed dominates the amplitude in such a way that

$$\sigma = \int_{M-2\Gamma}^{M+2\Gamma} dM_{WW} \frac{d\sigma}{dM_{WW}}, \tag{13}$$

where M and Γ are the characteristic parameters of the resonance obtained from the unitarized amplitudes.

We are now in disposition to compare our results from the unitarized analysis of σ next to the experimental ones. But first, two aspects need to be taken into account. Firstly, our analysis only says something about longitudinally polarized gauge bosons in the external states; any contribution coming from different polarization combinations is to be computed separately and with the corresponding effective luminosity. However, we expect the purely longitudinal process to dominate at high energies when we separate, even just a little, from the SM. If that is the case we should not saturate the experimental value which is unpolarized. Secondly, we can easily include in our calculation kinematical cuts on the pseudorapidity and the invariant mass of the outgoing gauge bosons but we can not demand restrictions in the kinematics of the radiated light jets suitable for VBS detection that are usually included in experimental analysis.

Taking into account all the machinery developed in this section to compute a theoretical cross section in pp collisions and the comments in the above paragraph, we can now compare with experimental results. In Fig. 3 we show values of the cross sections obtained using

[2]Other luminosity functions are available in the literature (see for example [20]). As soon as the experimental evidence of H (650) gets consolidated, it would good to consider all them for a deeper and more complete analysis.

Eq. (13) for a subset of the parameter space in Fig. 2 ($k \times \gamma = [0.1, 0.11] \times [0.0007, 0.001]$) where resonances with masses close to 650 GeV appear.

In Fig. 3, we show the values of the cross sections obtained for WW (left panel) and ZZ (right panel) final states at $\sqrt{s} =$ 13 TeV pp collision energy after VBS using Eq. (11). The cross sections for WW result to be of order ∼300 fb and ∼75 fb for ZZ for all values of k and γ. The measured cross sections from VBS [5] of $\mathrm{H}(650) \to WW$ and $\mathrm{H}(650) \to ZZ$ are 160 ± 50 fb and 30 ± 15 fb, respectively, close to SM values. These measurements really favor a WW scenario after VBF rather than a ZZ final state, with a ratio between cross sections $\sigma_{WW}/\sigma_{ZZ} \sim 5$. Our calculation implies $\sigma_{WW}/\sigma_{ZZ} \sim 4$, relatively close to the ATLAS and CMS analysis but really distant from the prediction using the Georgi-Machacek model, which infers the inverse situation with a ZZ final state dominating over the WW one with $\sigma_{WW}/\sigma_{ZZ} \sim 0.5$ [2,5].

We obtain with our calculation, thus, two times the measured central values. As explained before, no cuts, and actually no kinematical condition, are imposed in our calculation in Fig. 3 for a better comparison with the experiment so we would expect our computed cross section to exceed the measured one. We can easily introduce a cut in the pseudorapitidies of the final state gauge bosons that favors the identification of VBS events. In particular if we impose $|\eta_W| < 2$ [22] the cross sections are reduced to ∼275 fb and ∼70 fb for WW and ZZ processes, respectively, getting closer to the experimental data. Presumably, further cuts on the kinematical variables of the light jets produced after radiation of the gauge bosons triggering the VBS would point towards even closer cross sections.

To conclude this section we present a test of our calculation by making a comparison in the number of events obtained for a process using Monte Carlo (MC) techniques in Ref. [22]. In this work the authors reproduced the signal expected at the LHC for vector charged resonances emerging in the subprocess $WZ \to WZ$. The range of chiral parameters used lead to resonances in the mass range 1.5–2.5 TeV. For the event simulation at center of mass energy of $\sqrt{s} = 14$ TeV, the authors used a series of kinematical cuts both in the WZ bound state and in the radiated light jets. On one hand, we also introduce for a more reliable comparison the cut on the pseudorapidity $|\eta_W| < 2$ by integrating the partonic amplitude in the corresponding values of $\cos\theta$. On the other hand, we can not apply any cut on the light jets easily.

The number of events obtained from our calculation of the VBS cross section for a specific value of the integrated luminosity is $N_{\mathcal{L}} = \sigma \cdot \mathcal{L}$, where σ is the total cross section in Eq. (13). The results for both number of events, the MC simulation in Ref. [22] and our theoretical prediction, are gathered in Table I.

As expected and argued before, all our number of events exceed the ones obtained using a MC simulation due to the lack of extra kinematical cuts. We also observe that the heavier the vector resonance is the more accurate the calculation with respect the MC.

TABLE I. Number of MC events for three benchmark points BP1, P2, and BP3 in Ref. [22] that produce vector resonances for different values of the integrated luminosity $\mathcal{L}$ in units of fb^{-1}, $N_{\mathcal{L}}^{MC}$. The number of events obtained with our calculation is $N_{\mathcal{L}} = \sigma \cdot \mathcal{L}$.

	$M_V - \frac{i}{2}\Gamma_V$	N_{1000}^{MC}	N_{1000}
BP1	$1510 - \frac{i}{2}13$	488	904
BP2	$2092 - \frac{i}{2}20$	82	121
BP3	$2541 - \frac{i}{2}27$	30	31

V. CONCLUSIONS

Searches for light scalar states should be pursued since their existence could be understood as Higgs companions extending the SM and giving an explanation to its origin. Up to now, there are no clear discoveries but there is still room for this new physics to emerge in the high-luminosity phase of the LHC.

In this work we have seen that H(650) can be accommodated in the HEFT but it requires the cooperation of at least one more next-to-leading coupling (for which no relevant bounds exist) when the coefficients a_4 and a_5 are pushed to the limit of the experimentally allowed region. Further restrictions on them derived from experiment would probably hinder the viability of the tentative resonance H(650). The prediction for the width of this resonance also fits well with the preliminary experimental observations.

We computed within the EWA, the cross section for the production of a 650 GeV resonance in the vector boson fusion channel via $pp \to WW + X$ and compared it with the results in Ref. [5], assuming that the scalar state only decays in gauge bosons and not to any other two scalars. We also include a comparison between the number of events with a MC simulating a charged vector resonance in the process $WZ \to WZ$ [22].

The results we find are encouraging in the sense that the predicted cross section is relatively close to the experimental analyses performed by ATLAS and CMS. First, without taking into account any event selection cut we obtained cross sections of ∼300 fb and ∼75 fb for WW and ZZ final states, respectively. These results are obtained within the EWA and assuming that the peak dominates the cross section. After applying cuts on the pseudorapidty of the diboson state, the values of the cross sections are reduced to ∼275 fb and ∼70 fb for WW and ZZ states, respectively.

ACKNOWLEDGMENTS

We thank F. Richard for clarifications regarding the experimental status of H(650). We acknowledge financial

support from the State Agency for Research of the Spanish Ministry of Science and Innovation through the "Unit of Excellence María de Maeztu 2020–2023" award to the Institute of Cosmos Sciences (CEX2019-000918-M) and from PID2019-105614GB-C21, 2017-SGR-929, and 2021-SGR-249.

[1] A. Dobado and D. Espriu, Prog. Part. Nucl. Phys. **115**, 103813 (2020).
[2] H. Georgi and M. Machacek, Nucl. Phys. **B262**, 463 (1985).
[3] M. S. Chanowitz and M. Golden, Phys. Lett. **165B**, 105 (1985).
[4] J. F. Gunion and H. E. Haber, Phys. Rev. D **67**, 075019 (2003).
[5] A. Kundu, A. Le Yaouanc, P. Mondal, and F. Richard, in *2022 ECFA Workshop on e+e- Higgs/EW/Top Factories* (2022), arXiv:2211.11723.
[6] S. Afonin, Phys. Lett. B **840**, 137882 (2023).
[7] I. Asiáin, D. Espriu, and F. Mescia, Phys. Rev. D **105**, 015009 (2022).
[8] I. Asiáin, D. Espriu, and F. Mescia, Phys. Rev. D **107**, 115005 (2023).
[9] I. Rosell, A. Pich, and J. J. Sanz-Cillero, *Proc. Sci.*, ICHEP2020 (2021) 077 [arXiv:2010.08271].
[10] A. M. Sirunyan *et al.* (CMS Collaboration), J. High Energy Phys. 03 (2021) 257.
[11] G. Aad *et al.* (ATLAS Collaboration), J. High Energy Phys. 07 (2021) 005.
[12] P. Cea, Mod. Phys. Lett. A **34**, 1950137 (2019).
[13] P. Cea, arXiv:2210.01579.
[14] A. Adams, N. Arkani-Hamed, S. Dubovsky, A. Nicolis, and R. Rattazzi, J. High Energy Phys. 10 (2006) 014.
[15] A. M. Sirunyan *et al.* (CMS Collaboration), Phys. Lett. B **795**, 281 (2019).
[16] M. Aaboud *et al.* (ATLAS Collaboration), Phys. Rev. D **95**, 032001 (2017).
[17] A. M. Sirunyan *et al.* (CMS Collaboration), Phys. Lett. B **798**, 134985 (2019).
[18] S. Banik, A. Crivellin, S. Iguro, and T. Kitahara, arXiv:2303.11351.
[19] S. Dawson, Nucl. Phys. **B249**, 42 (1985).
[20] A. Alboteanu, W. Kilian, and J. Reuter, J. High Energy Phys. 11 (2008) 010.
[21] D. Espriu and B. Yencho, Phys. Rev. D **87**, 055017 (2013).
[22] R. L. Delgado, A. Dobado, D. Espriu, C. Garcia-Garcia, M. J. Herrero, X. Marcano, and J. J. Sanz-Cillero, J. High Energy Phys. 11 (2017) 098.